

Remote Cooling of Spin-ensembles Coupled to a Spin-mechanical Hybrid Interface

Yang Wang and Durga Dasari*

3. Physikalisches Institut, ZAQuant, University of Stuttgart, Allmandring 13, 70569 Stuttgart, Germany

We present here a protocol for the ground-state cooling of a hybrid quantum system consisting of a spin ensemble, an oscillator, and a single probe spin. In the weak dispersive coupling limit between the spins and the oscillator, a back-action effect from frequent measurements of the probe spin allows exponential cooling of the hybrid system. We identify the parameter regimes necessary to cool the ensemble, the oscillator, or both to their thermal ground states. Our results contribute to the development of a practical solution for cooling/polarizing large spin ensembles. More importantly, we show that even with weak coupling, significant changes in the dynamics of such ensemble-oscillator hybrid systems can be achieved by manipulating a single spin. This result provides a relatively simple means of tuning the dynamics of a hybrid system, which might facilitate advances in many quantum technology applications such as preparing entangled states in macroscopic objects.

I. INTRODUCTION

Quantum technology holds great potential to revolutionize areas such as information processing [1–3], secure communication [4, 5], sensing [6, 7], and fundamental testing [8]. However, translating this potential into real-world applications remains a significant challenge due to the inherent limitations of current experimental platforms [9, 10]. For example, nitrogen-vacancy (NV) centers in diamond [11] have an extended coherence time [12, 13] and an optical interface that enables long-range entanglement [14, 15], but their limited control accuracy [16] hinders advanced applications such as fault-tolerant quantum computation [17, 18]. Therefore, it is essential to explore the hybrid system approach that fully exploits the unique capabilities of different systems [19–22]. Following this idea, large NV ensembles have been used exclusively as memory for superconducting qubits [23, 24], known for their superior control fidelity [1], reducing the need for high-precision entangling gates over NV centers required for quantum computation. The rich dynamics of hybrid quantum systems also opens up significant prospects for sensing [22, 25], simulation [21, 26] and machine learning [27–29].

Establishing high-fidelity entanglement between remote spin qubits through a bus is a well-studied paradigm [22, 30]. The idea is to transduce their common coupling to macroscopic objects (bus) into indirect interactions that lead to their entanglement [30, 31]. Nano-mechanical oscillators have been playing a pivotal role in creating universal quantum transducers for spin–spin spin-photon and phonon-photon interactions [32, 33]. Other transducers in the form of magnons [34], superconducting qubits [35, 36], optical cavities [25], optomechanical cavities [37], and superconducting resonator [38] have also been considered. There is also a proposal of using a three-level spin as the transducer to mediate entanglement between two oscillators [39].

Transducers have primarily been proposed to create indirect interactions between the initially non-interacting systems, effectively implementing entanglement gates between remote qubits [33, 34, 37]. Nevertheless, there are few transducer protocols that focus on heat extraction from quantum systems to achieve ground state cooling or quantum state preparation. This aspect is crucial, especially for large spin ensembles, since conventional ensemble cooling or polarization techniques often rely on resonant energy exchange methods, such as the Hartman-Hahn transfer [40, 41].

Polarization based on energy transfer typically exploit the interaction between a single spin and all the ensemble spins. This single spin can be repeatedly polarized, thus realizing a continuous removal of entropy from the ensemble, leaving it finally polarized. However, when dealing with identical spins (with similar g-factors), the risk of the ensemble being trapped in dark states due to Hamiltonian symmetries is significantly high [41, 42], which prevents full polarization. This dark state problem can be overcome by performing projective measurements on a single qubit interacting with the target ensemble and using its back action to extract heat. Such quantum state projections of a single spin not only allow efficient heat extraction from an ensemble, but can also work in a non-trivial situation where the original system dynamics does not provide any energy exchange [43, 44].

In this work, we will consider a tripartite hybrid system consisting of a spin ensemble, an oscillator, and a single spin (probe). Since we envision the oscillator to be a macroscopic object such as a nano-mechanical oscillator, the probe spin and the ensemble can be remotely entangled, as schematically shown in Fig. 1. In the limit where the oscillator is dispersively coupled (off-resonant) to the probe and ensemble spins, no energy exchange is possible from the natural Hamiltonian dynamics. However, by exploiting the measurement back action from the frequently measured probe spin, it is possible to cool/polarize the spin ensemble from its initial fully mixed thermal states to the ground states.

Our cooling protocol is based on indirect coupling between the probe spin and the ensemble that is mediated by the oscillator. It has already been demonstrated that

* d.dasari@pi3.uni-stuttgart.de

multiple spins can be coupled to a nano-mechanical oscillator [43, 44], which would be much easier than achieving strong coupling between a single spin and all target spins in a large ensemble directly [24]. Moreover, since only weak dispersive coupling between the spins and the oscillator is required, our protocol can be straightforwardly implemented on a large variety of physical systems and is anticipated to be more feasible for cooling down larger electron-spin ensembles. Furthermore, given the wide operating temperature range of contemporary hybrid systems, from 4K to 300K, the need for cooling down individual components is paramount [45].

The paper is organized as follows: In Sec. II, we outline the Hamiltonian of the system and discuss possible experimental implementations of our proposal. In Sec. III, we analyze the dynamics of the hybrid system and describe how periodic dynamical decoupling (DD) pulses on the probe spin can modify the dynamics of other parts in the system. In Sec. V, we study the parameters that allow cooling of the spin ensemble, the oscillator, or both. Finally, Sec. VI provides a summary and discusses possible directions for future research.

II. SETUP

This work focuses on a tripartite quantum system consisting of an ancilla spin (probe), a spin ensemble, and an oscillator. This hybrid system can be realized as shown in Fig. 1 through a one-sided clamped cantilever embedding a single NV center positioned such that it experiences maximal strain coupling. To the edge of the cantilever is attached a magnetic tip that produces a field gradient ∇B . This field is then coupled to a spin ensemble on an external substrate. The spin ensemble and the probe spin are both coupled to the mechanical motion through the field gradients [22, 33] or longitudinal strain [46–48].

For simplicity, we assume (though not necessary) that the ensemble spins interact with the common mechanical mode uniformly with a coupling strength denoted as g . In addition, the probe spin is assumed to have a distinct coupling strength with the oscillator, denoted as g_0 .

The hybrid system's Hamiltonian is then formulated as follows:

$$H = \omega a^\dagger a + \sum_{k=0}^N \omega_k S_{k,z} + \left(g_0 S_{0,z} + g \sum_{k=1}^N S_{k,z} \right) (a + a^\dagger), \quad (1)$$

where $S_{i,z}$ signifies the z-component of the spin-1/2 operator for the i th spin, oscillating at the Larmor frequency ω_i . The oscillator's annihilation and creation operators are denoted by a and a^\dagger , with a frequency ω .

The single probe spin is envisioned to be solid state spins in diamond such as NV center electronic spins, due to good spin coherence properties, high degree spin control and a well-resolved optical spectrum at low temperatures [16, 17, 49]. The optical interface allows optical excitation to various levels that can either initialize or

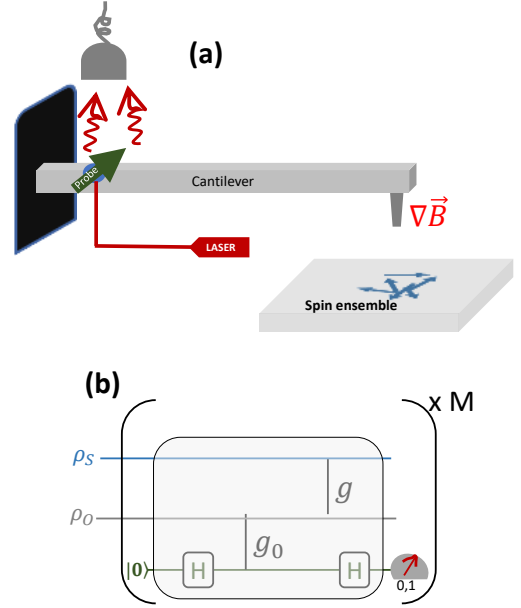


FIG. 1. (a) Schematic illustration of the control procedure detailed in the paper. (a) A clamped nano/micro-mechanical cantilever hosting single defect spin, that is coupled to its motion through strain and is manipulated by laser and RF fields. A magnetic tip attached at the edge of the cantilever produces a gradient field $\nabla \vec{B}$ on a nearby spin ensemble allowing for its coupling to the mechanical motion of the cantilever. (b) Schematic illustration of the coupling and control mechanism for the above described spin-mechanical system. While the probe spin (green) is reset (to state $|0\rangle$) after every projective measurement, the oscillator (ρ_0) and ensemble states (ρ_s) continue to evolve conditioned on the measurement of the probe.

readout the spin state with fidelities exceeding 98% [50]. In addition, these spins can also (weakly) couple to external spins, photons [43, 51] and phonons [37, 44].

Note that the NV electronic spin-1 can be operated as a qubit with its $m_s = 0, -1$ sub-levels by applying a 400 Gauss external magnetic field aligned with its symmetry axis to separate the $m_s = \pm 1$ levels [17]. Such an arrangement negates the need to consider transverse spin-strain coupling due to its direct interaction between the $m_s = \pm 1$ levels [30, 47, 48], so we can safely ignore the $m_s = +1$ sublevel in this work. What remains is the longitudinal strain coupling acting on the qubit levels. This number can be up to 10 kHz for NV centers [52], and higher for other defect centers [53].

The spin ensemble to be cooled can be chosen with more flexibility, as stringent control over these spins is not a prerequisite for the current study. Potential candidates for the spin ensemble include distant spins on other coupled cantilevers, spins at the clamped edge that are strain-coupled to the mechanical mode, or other surface electron spins. Even more complex would be the situation where the spins coupled to the mechanical mode

are not the spins attached to the NV centers in diamond but are dark (electronic) spins on the surface [54] of the NMO, or other ferromagnetic particles [55]. To harness those spins for spin-mechanics one should rely on indirect polarization techniques as they cannot be directly polarized optically. Note that, as schematically shown in Fig. 1(a), the interaction between the ensemble spins and the mechanical vibrational mode is generated by a magnetic tip attached to the cantilever with high field gradients. Here the coupling strength can be much higher [56], than the strain coupling between probe and the oscillator.

III. SYSTEM DYNAMICS

In the following, we will consider the system in the rotating frame of precession frequencies of the oscillator and the spins. The rotating-frame Hamiltonian reads

$$\tilde{H} = \left(g_0 S_{0,z} + g \sum_{k=1}^N S_{k,z} \right) (\hat{a} e^{-i\omega t} + \hat{a}^\dagger e^{i\omega t}). \quad (2)$$

Since the ensemble spins form a finite-dimensional Hilbert space, the system evolution operators can be written in the form [57, 58]:

$$U(t) = |0\rangle\langle 0| \otimes \sum_{k=0}^N \mathcal{D}_{k,+}(t) \otimes \mathbf{I}_k \\ + |1\rangle\langle 1| \otimes \sum_{n=0}^N \mathcal{D}_{n,-}(t) \otimes \mathbf{I}_n, \quad (3)$$

$$\mathcal{D}_{k,\pm}(t) = \mathcal{T} \exp \left(\pm i \int_0^t dt' h_{k,\pm}(t') \right),$$

where \mathcal{T} the time ordering operator, and \mathbf{I}_k projects the spin ensemble into the subspace where k spins are pointing up. For example, when $N = 3$ and $k = 2$, the projector is written as

$$\mathbf{I}_{k=2} = |\uparrow\uparrow\downarrow\rangle\langle\uparrow\uparrow\downarrow| + |\uparrow\downarrow\uparrow\rangle\langle\uparrow\downarrow\uparrow| + |\downarrow\uparrow\uparrow\rangle\langle\downarrow\uparrow\uparrow|. \quad (4)$$

The term $h_{k,\pm}(t)$ is hence the oscillator Hamiltonian conditioning on the states of the spins. It is expressed as

$$h_{k,\pm}(t) = \frac{g(k - N/2) \pm g_0}{2} (\hat{a} e^{-i\omega t} + \hat{a}^\dagger e^{i\omega t}). \quad (5)$$

It has been shown that the Magnus expansion of the evolution operators can be simplified as [57, 58]

$$\mathcal{D}_{k,\pm}(t) = \exp \left(\pm i \int_0^t dt' h_{k,\pm}(t') \right) \\ \times \exp \left(\frac{1}{2} \int_0^t dt' \int_0^{t'} dt'' [h_{k,\pm}(t'), h_{k,\pm}(t'')] \right) \\ = \exp \left[\frac{g(k - N/2) \pm g_0}{2\omega} (\alpha(t) a^\dagger - \alpha^*(t) a) \right] \\ \times \exp(i t \theta_k). \quad (6)$$

where the functions $\alpha(t)$, $\beta(t)$ and θ_k are given by

$$\alpha(t) = 1 - e^{i\omega t}, \quad \beta(t) = \frac{\omega t - \sin(\omega t)}{\omega t}, \quad (7) \\ \theta_k = -\beta(t) (g(k - N/2) \pm g_0)^2 / 4\omega.$$

IV. PROBE SPIN CONTROL

In addition to the natural dynamics induced by the spin-oscillator interaction given in Eq. (1), we also apply a periodic sequence of π pulses on the probe spin. These pulses significantly alter the dynamics of the system by embedding a time-periodic function $f(t)$ into the Hamiltonian, described as follows:

$$f(t) = \begin{cases} +1 & \text{if } 2j\tau < t < (2j+1)\tau \\ -1 & \text{if } (2j+1)\tau < t < (2j+2)\tau \end{cases} \quad (8)$$

where $j = 0, 1, 2, \dots, n$ and τ denotes the interval between successive pulses. By replacing g_0 with $f(t)g_0$ in $h_{k,\pm}(t)$, the conditional evolution operators in Eq (6) are now written as

$$\mathcal{D}_{k,\pm}^f(t) = \exp \left[\frac{g(k - N/2)}{2\omega} (\alpha(t) a^\dagger - \alpha^*(t) a) \right. \\ \left. \pm \frac{f(t)g_0}{2\omega} (F(\epsilon, t) a^\dagger - F^*(\epsilon, t) a) \right] \exp[i\theta_k(t)], \quad (9)$$

where the filter function $F(t)$ is given by [57]

$$F(t) = i\omega \sum_{k=0}^n \int_{k\tau}^{(k+1)\tau} dt (-1)^k e^{-i\omega t} \\ = - \sum_{k=0}^n (-1)^k \left[e^{-i(k+1)\omega\tau} - e^{-ik\omega\tau} \right] \\ = \left[1 - (-1)^{n+1} e^{-i(n+1)\omega\tau} + 2 \sum_{k=1}^n (-1)^k e^{-ik\omega\tau} \right]. \quad (10)$$

This filter function can be expressed in a well-known form, centered at $\tau = \pi/\omega$ and with its width decreasing approximately as $1/n^2$ [57–59]:

$$F^2(\tau, n, \omega) = 4 \tan^2 \left(\frac{\omega\tau}{2n+2} \right) \cos^2 \left(\frac{\omega(n+1)\tau}{2} \right), \quad (11)$$

The asymptotic behavior of the filter function is given by

$$\lim_{n \rightarrow \infty} F(t) = 2(n+1) \delta(\omega - \frac{\pi}{\tau}). \quad (12)$$

In practice, to ensure only the mode at the particular frequency π/τ couples to the probe spin, the number of pulses on the probe should be $n > \mathcal{O}(\omega/g_0)$. Other

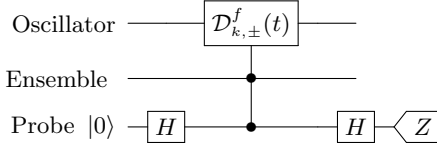


FIG. 2. Quantum circuit illustrating the implementation of a projector on the oscillator, influenced by the spin ensemble states and the measurement result of the probe spin. The process starts with the ancilla spin in the $|+\rangle$ state, followed by the application of repeated DD pulses. This leads to a $\mathcal{D}_{k,\pm}^f(t)$ controlled evolution guided by the spin ensemble P_k . The procedure ends with a $\pi/2$ pulse and measurement of the ancilla spin in the Pauli Z basis. The specific projector realized is expressed mathematically in Eq (15).

phonon modes are effectively decoupled [58], which supports our initial assumption of a single oscillator mode in Eq. (1).

Furthermore, our analysis focuses on the scenario where the inversion pulses resonate with the oscillator frequency. To achieve resonance, we set the interval between successive inversion pulses as

$$\tau = \frac{\pi}{\omega - \epsilon}, \text{ where } \frac{\epsilon}{\omega} \ll 1, \quad (13)$$

where the detuning parameter ϵ is intentionally kept significantly smaller than the oscillator frequency ω to facilitate near-resonant conditions. The filter function is now simplified to

$$F(\epsilon, t = (n+1)\tau) = 1 - e^{i\epsilon t} + \frac{2(1 - e^{i\epsilon t})}{e^{-i\epsilon\tau} - 1}. \quad (14)$$

In our investigation, we focus specifically on the weak dispersive coupling between each spin and the oscillator, deliberately ignoring any direct interactions between the spins. Nevertheless, by carefully choosing the detuning ϵ and the number of pulses n , substantial changes in the dynamics of the spin ensemble and the oscillator can be induced. The modification of the dynamics is facilitated by a cyclic process involving the projective measurement and reinitialization of the ancilla spin, as schematically depicted in Fig. 1. Initially, the ancilla spin is prepared in the state $|+\rangle$. Then the system undergoes a DD-modulated evolution for a time $t = n\tau$, as described in Eq (3). Finally, the probe spin is measured in the Pauli-Z basis, following the application of an additional $\pi/2$ pulse to it.

The process described above is represented by the circuit in Fig. 2. It leads to the implementation of a projector throughout the system depending on the probe measurement outcome, as mathematically formulated:

$$\mathcal{P}_{N,\pm} = \sum_{k=0}^N V_{k,\pm} \otimes \mathbf{I}_k, \quad V_{k,\pm} = \frac{1}{2} (\mathcal{D}_{k,+}^f(t) \pm \mathcal{D}_{k,-}^f(t)), \quad (15)$$

where $V_{k,\pm}$ is the projector on the oscillator, k is the number of ensemble spins pointing up, and \pm is the result of

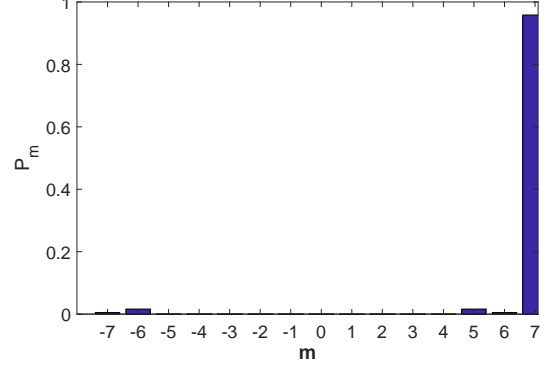


FIG. 3. We plot the probability of projecting a spin ensemble into its possible total magnetization states (from $-N/2$ to $N/2$) after repeated conditional measurements of the probe spin in the state $|0\rangle$, as described in Eq. (18). Here we consider an ensemble with $N = 14$ spins, an oscillator with frequency $\omega = 1.2\text{MHz}$ that is weakly coupled to the probe and spin ensembles with strengths of $g_0 = g = 10\text{kHz}$. The probe is modulated periodically with $n = 128$ π -pulses with an interval $\tau = \pi/\omega - \epsilon$. Here the detuning is set as $\epsilon = 1.1\text{kHz}$. The probability distribution reaches saturation after $M = 100$ measurements.

the ancilla measurement. The repeated application of such projectors is central to the cooling of the oscillator in our previous work [58], which is now extended to cooling/polarizing an entire spin ensemble in this work.

V. SYSTEM COOLING

In this section, we describe the protocol that imposes a thermal filter on the hybrid system, allowing for controlled cooling of either the oscillator, the spin ensemble, or both. We start with N spins in the ensemble, which are initially assumed to be in a fully mixed state, and the oscillator is assumed to be in its thermal state. These initial states are written as

$$\rho_{\text{ens}} = \sum_{k=0}^N \frac{\mathbf{I}_k}{2^N}, \quad \rho_{\text{osc}} = \frac{1}{\sum_n e^{-\frac{n\omega}{k_B T}}} \sum_n e^{-\frac{n\omega}{k_B T}} |n\rangle \langle n|. \quad (16)$$

Here the projector \mathbf{I}_k represents the states with k spins pointing up, as shown in Eq. (4); k_B represents the Boltzmann constant; and T is the temperature. The ensemble spins are fully unpolarized, i.e., $\langle \sum_{j=1}^N S_{z,j} \rangle = 0$; and the initial thermal occupancy of the oscillator is calculated as

$$n_0 = \text{Tr}(\rho_{\text{osc}} a^\dagger a) = \frac{1}{e^{(n\omega/k_B T)} - 1}. \quad (17)$$

Following the circuit depicted in Fig. 2, we measure the probe spin, selecting only outcomes of 0. This process

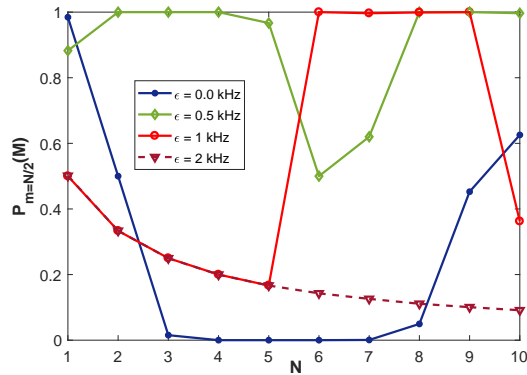


FIG. 4. Non-trivial dependence of the final maximum polarization on the detuning ϵ for varying spin-ensemble sizes (N). The y-axis represents the probability of finding all ensemble spins pointing up after $M = 100$ probe projection measurements, denoted as $P_{m=N/2}(M)$. Note that the oscillator frequency is set as $\omega = 1.2\text{MHz}$ and the spin-oscillator coupling strengths are set as $g_0 = g = 10\text{kHz}$.

effectively implements the projector $\mathcal{P}_{N,+}$ as defined in Eq. (15). Upon performing M such measurements, the probability that the ensemble is in the I_k sector is calculated as

$$P_m = \frac{1}{\sum_m P_m} \text{Tr}[\mathcal{P}_{N,+}^M \rho_B(0) \mathcal{P}_{N,+}^M], \quad (18)$$

where $m = (2k - N)/2$ is the total magnetization of the ensemble. This dependence on m shows that, with appropriate parameter choices, it is possible to achieve $P_{m=N/2} \approx 1$, thereby polarizing the ensemble. This ensemble polarization depends non-trivially on the filter function imposed by the pulses on the probe spin, as can be seen from Eq. (14). It gives us a new control parameter ϵ that would affect the projection of the spin ensemble onto different m -states.

In this work, we will focus on the weak coupling regime, i.e., $g \ll \omega$, and we choose the detuning $\epsilon \sim \mathcal{O}(g)$ [31] so that $\epsilon \ll \omega$. Specifically, we consider the case where the spin couplings g , g_0 are 10 kHz and the mechanical oscillation frequency is chosen to be 1.2 MHz. Consequently, for a spin ensemble of size $N = 14$, by fixing the detuning to be $\epsilon = 1.16$ kHz, one can see that the sector with all spins up ($m = 7$) is predominantly left, effectively polarizing the ensemble. To further illustrate the non-trivial dependence of the maximum ensemble polarization on the detuning ϵ , we vary its value from 0 to 2 kHz and also vary the number of ensemble spins. Note that we always assume $M = 100$ projections of the probe spin.

A critical factor in achieving ensemble polarization is to ensure that the interval between successive pulses on the probe is close to resonance, i.e., a negligible detuning, $\epsilon \approx 0$, as indicated in Eq. (13). The reason for this

is to prevent premature cooling of the oscillator, since its thermal occupancy significantly affects the interaction between the probe and the ensemble, as detailed in Eq. (1). To allow the oscillator to cool, the detuning must be set to a higher value to facilitate its rapid cooling [58].

In Fig. 5 we show a pulse sequence that polarizes an ensemble of $N = 4$ spins and cools an oscillator starting from an initial thermal occupancy of $n_0 = 45$. We first optimize the cooling of the spin-ensemble by varying the detuning, to find an optimal point $\epsilon_1 = 1.1\text{kHz}$ where the ensemble polarizes perfectly, while the oscillator occupancy remains unchanged. This behavior is similar to what one would expect for resonant case ($\epsilon = 0$). Now for another 50 probe measurements and shifting the detuning to a higher value of $\epsilon_2 = 5\text{kHz}$, would rapidly cool the oscillator as shown in the right part of Fig. 5. Shifting ϵ_2 to even higher values would require more inversion pulses on the probe to achieve a similar effect, as can be seen from Eq. (12). We would like to note that there would be no effect of the dephasing caused by the surrounding spin-bath on the cooling dynamics, as each measurement also partially collapses the spin-bath towards steady states that eventually stabilize the cooling mechanism [60]. Other noise sources only affect the cooling rates, but not the final steady states of the ensemble and the oscillator.

A subtle but crucial aspect of cooling the oscillator is to choose the detuning ϵ precisely so that the conditional displacement operator $D(\theta)$ in Fig. 2 is not perfectly aligned with the position quadrature. Note that when the detuning is zero, $D(\theta)$ is just perfectly aligned with the momentum quadrature. In both cases the oscillator cannot be cooled [58]. This observation is intriguingly related to Gottesman-Kitaev-Preskill (GKP) state encoding by phase estimation, which uses the same control of applying inversion pulses to the probe spin and its measurement. However, the detuning ϵ must now be carefully chosen for each measurement to ensure that the conditional oscillator displacement is exactly aligned with either the momentum or position quadratures. In addition, we must carefully tune the magnitude of the oscillator displacement. Starting with an oscillator in its zero photon ground state, this process actually increases the number of photons and allows the preparation of GKP states in the oscillator [61, 62].

In the Appendix A, we discuss this proposal in more detail, where it becomes clear that encoding GKP states in a nanomechanical oscillator would be much more challenging. This is because a much stronger spin-mechanical coupling strength is needed, since the coherence time of mechanical vibration is rather limited.

VI. DISCUSSION

In this research, we have emphasized the profound influence that the precise control of a single spin can have on the dynamics of ensemble oscillator systems, and demon-

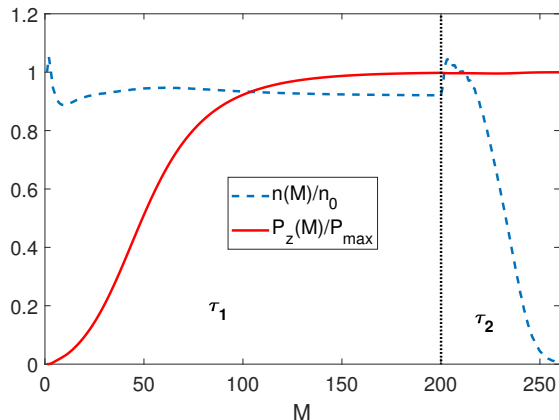


FIG. 5. Cooling the oscillator and spin ensemble. This figure shows the polarization P_z and the thermal occupancy $n(\omega)$ for both the spin ensemble and the oscillator, illustrating how the cooling/polarization progresses with the number of measurements M . The effective cooling of these quantum systems occurs in different parameter regimes. Initially, the spin ensemble is cooled by adjusting the π pulse intervals to near-resonance conditions, specifically τ_1 such that $\epsilon_1 = 0.11\text{kHz}$, where the thermal occupancy of the oscillator remains largely unaffected. After the spin ensemble has cooled, changing the pulse interval to τ_2 , which produces a more significant off-resonance with $\epsilon_2 = 1.5\text{kHz}$, leads to a rapid cooling of the oscillator to its ground state. The coupling parameters are also $g_0 = g = 10\text{kHz}$, with an oscillator frequency $\omega = 1.2\text{MHz}$. Here, we have considered an initial oscillator thermal occupation of $n_0 \approx 45$, and a spin ensemble size of $N = 4$ so that $P_{\max} = 2$.

strated this effect in the regime of weak coupling. This finding is central to a wide range of quantum technological applications. Specifically, we have introduced a ground-state cooling protocol for a tripartite hybrid quantum system that includes a spin ensemble, an oscillator, and a single probe spin. By exploiting the weak dispersive coupling between the spins and the oscillator, together with the feedback from frequent measurements of the probe spin, our protocol can cool both the spin ensemble and the oscillator to their ground states, either individually or in tandem.

Our numerical simulations over various parameter settings not only confirm the practicality of our cooling protocol, but also provide a basis for its experimental implementation. For example, our analysis shows that a spin ensemble of $N = 14$ spins could be cooled with a spin-mechanical coupling strength as low as 1 kHz at a mechanical oscillation frequency of about 1 MHz . Such coupling strengths, though are on the higher side of current state-of-the-art experiments, can become realizable by further reducing dimensions of the mechanical oscillator [63]. For other solid-state defects in silicon carbide, the coupling strengths could reach a few MHz [53], allowing us to attain higher cooling rates.

Another notable limitation of our cooling scheme is its

reliance on post-selection, which leads to an exponential decrease in success rate as the number of probe measurements increases. Nevertheless, our protocol offers a distinct advantage in its applicability to cooling large spin ensembles that are otherwise difficult to control and cannot be cooled by conventional optical or energy transfer methods. Furthermore, for spin ensembles that are amenable to such traditional cooling methods, such as NV centers in diamond, our approach adds to the toolbox and serves as a complementary polarization method. For example, optical methods could initially polarize an NV ensemble to a certain degree, after which our protocol could be used to further cool the ensemble toward the ground state, while maintaining a reasonable success rate. This will help us to alleviate the heating problem caused by intensive optical initialization.

Finally, this work also explores the potential of extending the cooling scheme to encode complex quantum states in oscillators, with a particular focus on the GKP states. Despite the important role of these states in quantum error correction [61, 62] and quantum sensing [64], their creation in macroscopic objects, such as a nanomechanical oscillator considered in this work, promises to deepen our understanding of the boundary between the classical and quantum worlds [65, 66]. Despite the inherent challenges, in particular the need for much stronger coupling strengths for experimental realization, our results provide insights for future efforts in this direction.

ACKNOWLEDGEMENT

The authors would like to thank Ruoming Peng and Jixing Zhang for feedback on the manuscript. This work is supported by German Federal Ministry of Education and Research (BMBF) for the project QECHQS under Grant No. 16KIS1590K.

Appendix A: Encoding a qubit into a macroscopic oscillator

In this section, we consider a hybrid system consisting of only the probe spin and the oscillator. We show that we can prepare a macroscopic mechanical oscillator in a complicated quantum state by controlling the probe. The exploration of such quantum superposition states in macroscopic objects has emerged as a significant area of interest, mainly because of its potential to explore the frontier between classical and quantum physics [65, 66].

Our proposal is realized by carefully tuning the detuning (ϵ) and applying a certain number of inversion pulses to the auxiliary spin. The quantum state in which we propose to place a macroscopic mechanical oscillator is the so-called Gottesman-Kitaev-Preskill (GKP) state [61, 67], which are defined as the simultaneous eigenstates

of the two stabilizers, i.e.,

$$S_q = e^{-i2\sqrt{\pi}\hat{p}}, S_p = e^{i2\sqrt{\pi}\hat{q}}. \quad (\text{A1})$$

The logical operators are correspondingly given by $X_L = \sqrt{S_p}$ and $Z_L = \sqrt{S_q}$, respectively.

However, the ideal GKP states are unphysical, requiring infinite amount of energy to prepare [61]. Instead, we will consider the approximate GKP states that are defined as (up to normalization):

$$\begin{aligned} |\tilde{0}\rangle &\propto \sum_{s=-\infty}^{\infty} \int_{-\infty}^{\infty} e^{-\frac{\Delta^2}{2}(2s)^2\pi} e^{-\frac{1}{2\Delta^2}(q-2s\sqrt{\pi})^2} |q\rangle dq, \\ |\tilde{1}\rangle &\propto \sum_{s=-\infty}^{\infty} \int_{-\infty}^{\infty} e^{-\frac{\Delta^2}{2}(2s+1)^2\pi} e^{-\frac{1}{2\Delta^2}(q-(2s+1)\sqrt{\pi})^2} |q\rangle dq. \end{aligned} \quad (\text{A2})$$

Note that the closer the squeezing parameter Δ is to 0, the higher is the quality of the GKP states [61, 67].

The GKP code is a promising candidate for quantum error correction (QEC) in continuous variable systems [68], such as photonic systems and cavity modes. In addition, GKP states hold promise for enhanced sensing capabilities, allowing simultaneous detection of an oscillator's displacements in both its position and momentum quadratures [64].

1. Oscillator displacements along the momentum and position quadratures

In the following, we assume that the spin ensemble is effectively decoupled from the rest of the system. The projectors given in Eq. (15) will then become just a displacement operator of the oscillator conditioning on the measurement result of the probe spin, as indicated by:

$$\mathcal{P}_{N=0,\pm} = \frac{D(\theta) \pm e^{i\phi} D(-\theta)}{2}, \quad (\text{A3})$$

where $D(\theta) = \exp(\theta a^\dagger - \theta^* a)$ represents the displacement operator, with the amplitude $\theta = g_0 F(\epsilon, t)/2\omega$.

The additional phase ϕ is introduced by rotating the ancilla spin by an angle ϕ before the measurement, as shown in the circuit in Fig. 6. The angle ϕ selects the effective measurement basis of the ancilla spin.

The proposed GKP encoding scheme involves repeated execution of this circuit, adaptively setting the ϕ angle based on previous measurement results. This is a phase estimation protocol that incrementally identifies the eigenvalue of $D(2\theta)$ while simultaneously projecting the oscillator into the corresponding eigenstate.

Displacement along position quadrature

For $\epsilon = 0$, the filter function simplifies to $F(\epsilon, t) = 2(n+2)$ so that $\theta = g_0 t/\pi$. This leads to conditional

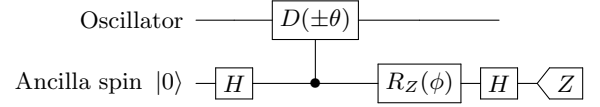


FIG. 6. Single round of an adaptive phase estimation protocol that estimates the eigenvalue of oscillator displacement operator, $D(2\theta) = \exp(2\theta a^\dagger - 2\theta^* a)$ with amplitude $2\theta = g_0 F(\epsilon, t)/\omega$. Initially, the ancillary spin is set in the $|+\rangle$ state and subsequently measured in the x-basis after applying a series of periodic inversion pulses, which facilitates the implementation of controlled oscillator displacements. Before measuring the ancilla spin, it undergoes a z-axis rotation by an angle ϕ . This angle ϕ is strategically determined based on the ancilla measurement results of previous phase estimation cycles, with the goal of minimize the uncertainty in the posterior probability distribution estimate of $D(2\theta)$'s eigenvalue. Specifically, when $\phi = 0$, this circuit simply executes the projectors given in Eq. (A3). Through repeated application of this phase estimation circuit, the oscillator states outside the subspace spanned by the eigenstates of $D(2\theta)$ are gradually suppressed.

displacements exactly along the position quadrature:

$$D(\theta) = \exp\left[\mp i \frac{\sqrt{2}g_0 t}{\pi} \hat{p}\right], \text{ with } \epsilon = 0, \quad (\text{A4})$$

where $\hat{p} = \frac{i}{\sqrt{2}}(\hat{a} - \hat{a}^\dagger)$ denotes the momentum operator of the oscillator. According to Ref. [33], this ability to adjust the oscillator's momentum based on the spin state facilitates a mechanism for entangling two spins by the oscillator.

Displacement along momentum quadrature

Additionally, we also need to realize controlled oscillator-displacements along the momentum quadrature. This is achieved by setting $\epsilon = \omega/(n+1)$ so that $\epsilon t = \pi$, the filter function reads

$$F(\epsilon, t) = 2 + \frac{4}{e^{i\epsilon t} - 1} = \frac{4}{i\epsilon t} + \mathcal{O}(\epsilon t), \quad (\text{A5})$$

where $\hat{q} = \frac{1}{\sqrt{2}}(\hat{a} + \hat{a}^\dagger)$ is the position operator of the oscillator. Correspondingly, we have $\theta = ig_0 t(n+1)/\pi^2(n+2)$. Furthermore, neglecting the higher order terms of $\epsilon t \sim \mathcal{O}(1/n)$ leads to the following displacement operator of the oscillator:

$$D(\theta) = \exp\left[\mp i \frac{2\sqrt{2}g_0 t}{\pi^2} \frac{n+1}{n+2} \hat{q}\right], \text{ with } \epsilon = \frac{\omega}{n+1}. \quad (\text{A6})$$

State preparation via phase estimation

Phase estimation has been shown to be effective for preparing such approximate GKP logical states by determining the eigenvalues of stabilizers and logical operators [62]. For the spin-oscillator hybrid system considered here, such eigenvalue determination is realized by

adjusting the detuning magnitude ϵ and the total evolution duration t . In this way, we can choose the magnitude by which the oscillator is shifted along the momentum or position quadrature.

For example, to prepare the approximate GKP state $|\bar{0}\rangle$, first initialize the oscillator in its ground state with zero photons. It then sets $D(\theta) = S_q$ and runs the phase estimation circuit several times to estimate its eigenvalue with high confidence. A subsequent fit to $D(\theta) = Z_L$ allows for similar eigenvalue estimation. Determining the eigenvalues of S_q and Z_L projects the oscillator into the desired approximate GKP state. This process can be described as iterative and adaptive application of the circuit in Fig. 6.

GKP encoding and oscillator cooling

The GKP encoding scheme we discuss is similar to the oscillator cooling technique described in Ref. [58], with both methods using the phase estimation circuit shown in Fig. 6 many times. However, the encoding scheme starts from the ground state, as opposed to the cooling method, which applies the circuit to a thermal state and then cools it down to the ground state.

A crucial difference between the two lies in how the circuit is used in the cooling process, where it is implemented with non-zero detuning, so that neither Eq.(16) nor Eq.(18) hold. When these conditions are satisfied, instead of cooling to a zero photon ground state, the oscillator, initially in a thermal state, stabilizes in a state that maintains a finite number of photons [58].

2. Experimental feasibility

In contrast to the oscillator cooling scheme developed in Ref. [58], which requires only a weak ancilla-oscillator

coupling, the GKP encoding scheme is much more demanding as it requires a strong coupling strength. Current experimental configurations are clearly inadequate in this regard to implement the preparation scheme. Furthermore, the GKP encoding scheme has been extensively studied in Ref. [62].

Therefore, we choose not to perform detailed numerical simulations to evaluate the practicality of the GKP encoding scheme in this study. Instead, we briefly assess the challenges and discuss potential improvements to existing setups that could facilitate the preparation of GKP states in macroscopic mechanical oscillators. The time duration for each phase estimation round needs to be of the order of $1/g_0$, so that the displacement magnitude can be of the order of $|\theta| \sim O(\sqrt{\pi})$. Given the necessity of around 10 phase estimation cycles to yield an approximate GKP state of acceptable quality [62], the preparation scheme requires an overall time exceeding $\mathcal{O}(10/g_0)$.

From an experimental point of view, it's crucial that the coherence time of the oscillator is considerably long compared to the coupling strength g_0 , ideally at least on the order of $100/g_0$. Diamond NMO with a quality factor $Q > 10^6$ have been demonstrated at sub-Kelvin temperatures and mechanical damping rates of about a few kHz [69]. This implies that the oscillator coherence time needs to be significantly improved. Note that the coherence time of the NV electronic spin in cryogenic conditions can exceed 1 second through the application of dynamical decoupling [12]. This is far from sufficient, as the probe spin only needs to maintain coherence during each phase estimation round.

[1] R. Acharya, I. Aleiner, R. Allen, T. I. Andersen, M. Ansmann, F. Arute, K. Arya, A. Asfaw, J. Atalaya, R. Babush, D. Bacon, J. C. Bardin, J. Basso, A. Bengtsson, S. Boixo, G. Bortoli, A. Bourassa, J. Bovaird, L. Brill, M. Broughton, B. B. Buckley, D. A. Buell, T. Burger, B. Burkett, N. Bushnell, Y. Chen, Z. Chen, B. Chiaro, J. Cogan, R. Collins, P. Conner, W. Courtney, A. L. Crook, B. Curtin, D. M. Debroy, A. Del Toro Barba, S. Demura, A. Dunsworth, D. Eppens, C. Erickson, L. Faoro, E. Farhi, R. Fatemi, L. Flores Burgos, E. Forati, A. G. Fowler, B. Foxen, W. Giang, C. Gidney, D. Gilboa, M. Giustina, A. Grajales Dau, J. A. Gross, S. Habegger, M. C. Hamilton, M. P. Harrigan, S. D. Harrington, O. Higgott, J. Hilton, M. Hoffmann, S. Hong, T. Huang, A. Huff, W. J. Huggins, L. B. Ioffe, S. V. Isakov, J. Iveland, E. Jeffrey, Z. Jiang, C. Jones, P. Juhas, D. Kafri, K. Kechedzhi, J. Kelly, T. Khatkar, M. Khezri, M. Kieferová, S. Kim, A. Kitaev, P. V. Klimov, A. R.

Klots, A. N. Korotkov, F. Kostritsa, J. M. Kreikebaum, D. Landhuis, P. Laptev, K.-M. Lau, L. Laws, J. Lee, K. Lee, B. J. Lester, A. Lill, W. Liu, A. Locharla, E. Lucero, F. D. Malone, J. Marshall, O. Martin, J. R. McClean, T. McCourt, M. McEwen, A. Megrant, B. Meurer Costa, X. Mi, K. C. Miao, M. Mohseni, S. Montazeri, A. Morvan, E. Mount, W. Mruczkiewicz, O. Naaman, M. Neeley, C. Neill, A. Nersisyan, H. Neven, M. Newman, J. H. Ng, A. Nguyen, M. Nguyen, M. Y. Niu, T. E. O'Brien, A. Opremcak, J. Platt, A. Petukhov, R. Potter, L. P. Pryadko, C. Quintana, P. Roushan, N. C. Rubin, N. Saei, D. Sank, K. Sankaragomathi, K. J. Satzinger, H. F. Schurkus, C. Schuster, M. J. Shearn, A. Shorter, V. Shvarts, J. Skrzynny, V. Smelyanskiy, W. C. Smith, G. Sterling, D. Strain, M. Szalay, A. Torres, G. Vidal, B. Villalonga, C. Vollgraf, Heidweiller, T. White, C. Xing, Z. J. Yao, P. Yeh, J. Yoo, G. Young, A. Zalcman, Y. Zhang, and N. Zhu, Suppressing quantum er-

- rors by scaling a surface code logical qubit, *Nature* **614**, 676 (2023).
- [2] D. Bluvstein, S. J. Evered, A. A. Geim, S. H. Li, H. Zhou, T. Manovitz, S. Ebadi, M. Cain, M. Kalinowski, D. Hangleiter, J. P. Bonilla Ataides, N. Maskara, I. Cong, X. Gao, P. Sales Rodriguez, T. Karolyshyn, G. Semeghini, M. J. Gullans, M. Greiner, V. Vuletić, and M. D. Lukin, Logical quantum processor based on reconfigurable atom arrays, *Nature* **626**, 58 (2023).
 - [3] J. Cai, A. Retzker, F. Jelezko, and M. B. Plenio, A large-scale quantum simulator on a diamond surface at room temperature, *Nat. Phys.* **9**, 168 (2013).
 - [4] S. Wehner, D. Elkouss, and R. Hanson, Quantum internet: A vision for the road ahead, *Science* **362**, 10.1126/science.aam9288 (2018).
 - [5] W. Zhang, T. van Leent, K. Redeker, R. Garthoff, R. Schwonnek, F. Fertig, S. Eppelt, W. Rosenfeld, V. Scarani, C. C.-W. Lim, and H. Weinfurter, A device-independent quantum key distribution system for distant users, *Nature* **607**, 687 (2022).
 - [6] N. Aslam, H. Zhou, E. K. Urbach, M. J. Turner, R. L. Walsworth, M. D. Lukin, and H. Park, Quantum sensors for biomedical applications, *Nat. Rev. Phys.* **5**, 157 (2023).
 - [7] F. Shi, Q. Zhang, P. Wang, H. Sun, J. Wang, X. Rong, M. Chen, C. Ju, F. Reinhard, H. Chen, J. Wrachtrup, J. Wang, and J. Du, Single-protein spin resonance spectroscopy under ambient conditions, *Science* **347**, 1135 (2015).
 - [8] B. Hensen, H. Bernien, A. E. Dréau, A. Reiserer, N. Kalb, M. S. Blok, J. Ruitenber, R. F. L. Vermeulen, R. N. Schouten, C. Abellán, W. Amaya, V. Pruneri, M. W. Mitchell, M. Markham, D. J. Twitchen, D. Elkouss, S. Wehner, T. H. Taminiau, and R. Hanson, Loophole-free bell inequality violation using electron spins separated by 1.3 kilometres, *Nature* **526**, 682 (2015).
 - [9] F. Battistel, C. Chamberland, K. Johar, R. W. J. Overwater, F. Sebastiano, L. Skoric, Y. Ueno, and M. Usman, Real-time decoding for fault-tolerant quantum computing: progress, challenges and outlook, *Nano Futures* **7**, 032003 (2023).
 - [10] V. Lordi and J. M. Nichol, Advances and opportunities in materials science for scalable quantum computing, *MRS Bulletin* **46**, 589 (2021).
 - [11] Y. Wang, *Using spins in diamond for quantum technologies*, Ph.D. thesis, Delft University of Technology (2023).
 - [12] M. H. Abobeih, J. Cramer, M. A. Bakker, N. Kalb, M. Markham, D. J. Twitchen, and T. H. Taminiau, One-second coherence for a single electron spin coupled to a multi-qubit nuclear-spin environment, *Nat. Commun.* **9**, 10.1038/s41467-018-04916-z (2018).
 - [13] B. D. Wood, G. A. Stimpson, J. E. March, Y. N. D. Lekhai, C. J. Stephen, B. L. Green, A. C. Frangeskou, L. Ginés, S. Mandal, O. A. Williams, and G. W. Morley, Long spin coherence times of nitrogen vacancy centers in milled nanodiamonds, *Phys. Rev. B* **105**, 205401 (2022).
 - [14] S. L. N. Hermans, M. Pompili, H. K. C. Beukers, S. Baier, J. Borregaard, and R. Hanson, Qubit teleportation between non-neighbouring nodes in a quantum network, *Nature* **605**, 663 (2022).
 - [15] M. Pompili, S. L. N. Hermans, S. Baier, H. K. C. Beukers, P. C. Humphreys, R. N. Schouten, R. F. L. Vermeulen, M. J. Tiggeleman, L. dos Santos Martins, B. Dirkse, S. Wehner, and R. Hanson, Realization of a multinode quantum network of remote solid-state qubits, *Science* **372**, 259 (2021).
 - [16] C. E. Bradley, J. Randall, M. H. Abobeih, R. C. Berrevoets, M. J. Degen, M. A. Bakker, M. Markham, D. J. Twitchen, and T. H. Taminiau, A ten-qubit solid-state spin register with quantum memory up to one minute, *Phys. Rev. X* **9**, 031045 (2019).
 - [17] M. H. Abobeih, Y. Wang, J. Randall, S. J. H. Loenen, C. E. Bradley, M. Markham, D. J. Twitchen, B. M. Terhal, and T. H. Taminiau, Fault-tolerant operation of a logical qubit in a diamond quantum processor, *Nature* **606**, 884 (2022).
 - [18] G. Waldherr, Y. Wang, S. Zaiser, M. Jamali, T. Schulte-Herbrüggen, H. Abe, T. Ohshima, J. Isoya, J. F. Du, P. Neumann, and J. Wrachtrup, Quantum error correction in a solid-state hybrid spin register, *Nature* **506**, 204 (2014).
 - [19] Z.-L. Xiang, S. Ashhab, J. Q. You, and F. Nori, Hybrid quantum circuits: Superconducting circuits interacting with other quantum systems, *Rev. Mod. Phys.* **85**, 623 (2013).
 - [20] G. Kurizki, P. Bertet, Y. Kubo, K. Mølmer, D. Petrosyan, P. Rabl, and J. Schmiedmayer, Quantum technologies with hybrid systems, *Proc. Natl. Acad. Sci.* **112**, 3866 (2015).
 - [21] X.-L. Hei, P.-B. Li, X.-F. Pan, and F. Nori, Enhanced tripartite interactions in spin-magnon-mechanical hybrid systems, *Phys. Rev. Lett.* **130**, 073602 (2023).
 - [22] S. Kolkowitz, A. C. Bleszynski Jayich, Q. P. Unterreithmeier, S. D. Bennett, P. Rabl, J. G. E. Harris, and M. D. Lukin, Coherent sensing of a mechanical resonator with a single-spin qubit, *Science* **335**, 1603 (2012).
 - [23] D. Marcos, M. Wubs, J. M. Taylor, R. Aguado, M. D. Lukin, and A. S. Sørensen, Coupling nitrogen-vacancy centers in diamond to superconducting flux qubits, *Phys. Rev. Lett.* **105**, 210501 (2010).
 - [24] X. Zhu, S. Saito, A. Kemp, K. Kakuyanagi, S.-i. Karimoto, H. Nakano, W. J. Munro, Y. Tokura, M. S. Everitt, K. Nemoto, M. Kasu, N. Mizuochi, and K. Semba, Coherent coupling of a superconducting flux qubit to an electron spin ensemble in diamond, *Nature* **478**, 221 (2011).
 - [25] L. Xie, Z. Yan, L. Wang, D. Wang, J. Liu, Y. Song, W. Xiong, and M. Wang, Unitary and efficient spin squeezing in cavity optomechanics, *arXiv:2401.15553* (2024).
 - [26] F. Fedele, F. Cerisola, L. Bresque, F. Vigneau, J. Monsel, J. Tabanera, K. Aggarwal, J. Dexter, S. Sevitz, J. Dunlop, A. Auffèves, J. Parrondo, A. Pályi, J. Anders, and N. Ares, Coupling a single spin to high-frequency motion, *arXiv:2402.19288* (2024).
 - [27] L. Körber, C. Heins, T. Hula, J.-V. Kim, S. Thlang, H. Schultheiss, J. Fassbender, and K. Schultheiss, Pattern recognition in reciprocal space with a magnon-scattering reservoir, *Nat. Commun.* **14**, 10.1038/s41467-023-39452-y (2023).
 - [28] K. Fujii and K. Nakajima, Harnessing disordered-ensemble quantum dynamics for machine learning, *Phys. Rev. Appl.* **8**, 024030 (2017).
 - [29] M. Negoro, K. Mitarai, K. Fujii, K. Nakajima, and M. Kitagawa, Machine learning with controllable quantum dynamics of a nuclear spin ensemble in a solid, *arXiv:1806.10910* (2018).
 - [30] P. Rabl, S. J. Kolkowitz, F. H. L. Koppens, J. G. E. Harris, P. Zoller, and M. D. Lukin, A quantum spin trans-

- ducer based on nanoelectromechanical resonator arrays, *Nat. Phys.* **6**, 602 (2010).
- [31] D. D. Bhaktavatsala Rao, N. Bar-Gill, and G. Kurizki, Generation of macroscopic superpositions of quantum states by linear coupling to a bath, *Phys. Rev. Lett.* **106**, 010404 (2011).
- [32] J. Bochmann, A. Vainsencher, D. D. Awschalom, and A. N. Cleland, Nanomechanical coupling between microwave and optical photons, *Nat. Phys.* **9**, 712 (2013).
- [33] E. Rosenfeld, R. Riedinger, J. Gieseler, M. Schuetz, and M. D. Lukin, Efficient entanglement of spin qubits mediated by a hot mechanical oscillator, *Phys. Rev. Lett.* **126**, 250505 (2021).
- [34] M. Fukami, J. C. Marcks, D. R. Candido, L. R. Weiss, B. Soloway, S. E. Sullivan, N. Deegan, F. J. Heremans, M. E. Flatté, and D. D. Awschalom, Magnon-mediated qubit coupling determined via dissipation measurements, *Proc. Natl. Acad. Sci.* **121**, 10.1073/pnas.2313754120 (2024).
- [35] Y. Wang and B. M. Terhal, Preparing dicke states in a spin ensemble using phase estimation, *Phys. Rev. A* **104**, 032407 (2021).
- [36] H. Hakoshima and Y. Matsuzaki, Efficient detection of inhomogeneous magnetic fields from a single spin with dicke states, *Phys. Rev. A* **102**, 042610 (2020).
- [37] R. Peng, X. Wu, Y. Wang, J. Zhang, J. Geng, D. Dasari, A. N. Cleland, and J. Wrachtrup, Spin-phonon entanglement in sic optomechanical quantum oscillators (2024), manuscript in preparation.
- [38] J. Dijkema, X. Xue, P. Harvey-Collard, M. Rimbach-Russ, S. L. de Snoo, G. Zheng, A. Sammak, G. Scappucci, and L. M. K. Vandersypen, Two-qubit logic between distant spins in silicon, *arXiv:2310.16805* (2023).
- [39] Q. Ansel, A. D. Chepelianskii, and J. Lages, Enhancing quantum exchanges between two oscillators, *Phys. Rev. A* **107**, 042609 (2023).
- [40] S. R. Hartmann and E. L. Hahn, Nuclear double resonance in the rotating frame, *Phys. Rev.* **128**, 2042 (1962).
- [41] D. D. B. Rao, A. Ghosh, D. Gelbwaser-Klimovsky, N. Bar-Gill, and G. Kurizki, Spin-bath polarization via disentanglement, *New J. Phys.* **22**, 083035 (2020).
- [42] K. Sasaki and E. Abe, Suppression of pulsed dynamic nuclear polarization by many-body spin dynamics, *Phys. Rev. Lett.* **132**, 106904 (2024).
- [43] S. Yang, Y. Wang, D. D. B. Rao, T. Hien Tran, A. S. Momenzadeh, M. Markham, D. J. Twitchen, P. Wang, W. Yang, R. Stöhr, P. Neumann, H. Kosaka, and J. Wrachtrup, High-fidelity transfer and storage of photon states in a single nuclear spin, *Nat. Photonics* **10**, 507 (2016).
- [44] A. Browaeys and T. Lahaye, Many-body physics with individually controlled rydberg atoms, *Nat. Phys.* **16**, 132 (2020).
- [45] M. Aspelmeyer, T. J. Kippenberg, and F. Marquardt, Cavity optomechanics, *Rev. Mod. Phys.* **86**, 1391 (2014).
- [46] P. Rabl, S. J. Kolkowitz, F. H. L. Koppens, J. G. E. Harris, P. Zoller, and M. D. Lukin, A quantum spin transducer based on nanoelectromechanical resonator arrays, *Nat. Phys.* **6**, 602 (2010).
- [47] S. D. Bennett, N. Y. Yao, J. Otterbach, P. Zoller, P. Rabl, and M. D. Lukin, Phonon-induced spin-spin interactions in diamond nanostructures: Application to spin squeezing, *Phys. Rev. Lett.* **110**, 156402 (2013).
- [48] A. Barfuss, J. Teissier, E. Neu, A. Nunnenkamp, and P. Maletinsky, Strong mechanical driving of a single electron spin, *Nat. Phys.* **11**, 820 (2015).
- [49] L. Robledo, L. Childress, H. Bernien, B. Hensen, P. F. A. Alkemade, and R. Hanson, High-fidelity projective readout of a solid-state spin quantum register, *Nature* **477**, 574 (2011).
- [50] N. Aslam, M. Pfender, P. Neumann, R. Reuter, A. Zappe, F. Fávoro de Oliveira, A. Denisenko, H. Sumiya, S. Onoda, J. Isoya, and J. Wrachtrup, Nanoscale nuclear magnetic resonance with chemical resolution, *Science* **357**, 67 (2017).
- [51] R. Chikkaraddy, V. A. Turek, N. Kongsuwan, F. Benz, C. Carnegie, T. van de Goor, B. de Nijs, A. Demetriadou, O. Hess, U. F. Keyser, and J. J. Baumberg, Mapping nanoscale hotspots with single-molecule emitters assembled into plasmonic nanocavities using dna origami, *Nano Lett.* **18**, 405 (2017).
- [52] S. D. Bennett, N. Y. Yao, J. Otterbach, P. Zoller, P. Rabl, and M. D. Lukin, Phonon-induced spin-spin interactions in diamond nanostructures: Application to spin squeezing, *Phys. Rev. Lett.* **110**, 156402 (2013).
- [53] S. J. Whiteley, G. Wolfowicz, C. P. Anderson, A. Bourassa, H. Ma, M. Ye, G. Koolstra, K. J. Satzinger, M. V. Holt, F. J. Heremans, A. N. Cleland, D. I. Schuster, G. Galli, and D. D. Awschalom, Spin-phonon interactions in silicon carbide addressed by gaussian acoustics, *Nature Physics* **15**, 490–495 (2019).
- [54] P. Huillery, T. Delord, L. Nicolas, M. Van Den Bossche, M. Perdriat, and G. Hétet, Spin mechanics with levitating ferromagnetic particles, *Phys. Rev. B* **101**, 134415 (2020).
- [55] W. K. Schomburg, *Introduction to Microsystem Design* (Springer Berlin Heidelberg, 2011).
- [56] F. Fung, E. Rosenfeld, J. D. Schaefer, A. Kabcenell, J. Gieseler, T. X. Zhou, T. Madhavan, N. Aslam, A. Yacoby, and M. D. Lukin, Programmable quantum processors based on spin qubits with mechanically-mediated interactions and transport (2023).
- [57] G. S. Agarwal, Saving entanglement via a nonuniform sequence of π pulses, *Phys. Scr.* **82**, 038103 (2010).
- [58] D. D. B. Rao, S. A. Momenzadeh, and J. Wrachtrup, Heralded control of mechanical motion by single spins, *Phys. Rev. Lett.* **117**, 077203 (2016).
- [59] G. S. Uhrig, Keeping a quantum bit alive by optimized pi-pulse sequences, *Phys. Rev. Lett.* **98**, 100504 (2007).
- [60] D. B. R. Dasari, S. Yang, A. Chakrabarti, A. Finkler, G. Kurizki, and J. Wrachtrup, Anti-zeno purification of spin baths by quantum probe measurements, *Nat. Commun* **13**, 10.1038/s41467-022-35045-3 (2022).
- [61] D. Gottesman, A. Kitaev, and J. Preskill, Encoding a qubit in an oscillator, *Phys. Rev. A* **64**, 012310 (2001).
- [62] B. M. Terhal and D. Weigand, Encoding a qubit into a cavity mode in circuit QED using phase estimation, *Phys. Rev. A* **93**, 012315 (2016).
- [63] T. M. Babinec, B. J. M. Hausmann, M. Khan, Y. Zhang, J. R. Maze, P. R. Hemmer, and M. Lončar, A diamond nanowire single-photon source, *Nat. Nanotechnol* **5**, 195–199 (2010).
- [64] K. Duivenvoorden, B. M. Terhal, and D. Weigand, Single-mode displacement sensor, *Phys. Rev. A* **95**, 012305 (2017).
- [65] C. Flühmann, T. L. Nguyen, M. Marinelli, V. Negnevitsky, K. Mehta, and J. P. Home, Encoding a qubit in a trapped-ion mechanical oscillator, *Nature* **566**, 513

- (2019).
- [66] M. Bild, M. Fadel, Y. Yang, U. von Lüpke, P. Martin, A. Bruno, and Y. Chu, Schrödinger cat states of a 16-microgram mechanical oscillator, *Science* **380**, 274 (2023).
 - [67] Y. Wang, *Quantum Error Correction with the GKP Code and Concatenation with Stabilizer Codes*, Master's thesis, RWTH-AACHEN UNIVERSITY (2017).
 - [68] C. Vuillot, H. Asasi, Y. Wang, L. P. Pryadko, and B. M. Terhal, Quantum error correction with the toric gottesman-kitaev-preskill code, *Phys. Rev. A* **99**, 032344 (2019).
 - [69] Y. Tao, J. M. Boss, B. A. Moores, and C. L. Degen, Single-crystal diamond nanomechanical resonators with quality factors exceeding one million, *Nat. Commun* **5**, 10.1038/ncomms4638 (2014).